Irrigation requirement estimation using MODIS vegetation indices and inverse biophysical modeling; A Case Study for Oran, Algeria

L. Bounoua, M. L. Imhoff and S. Franks
Submitted to Remote Sensing of the Environment-RSE
Popular Summary

Human demand for food influences the water cycle through diversion and extraction of fresh water needed to support agriculture. Future population growth and economic development alone will substantially increase water demand and much of it for agricultural uses.

For many semi-arid lands, socio-economic shifts are likely to exacerbate changes in climate as a driver of future water supply and demand. For these areas in particular, where the balance between water supply and demand is fragile, variations in regional climate can have potentially predictable effect on agricultural production. Satellite data and biophysically-based models provide a powerful method to quantify the interactions between local climate, plant growth and water resource requirements. In irrigated agricultural lands, satellite observations indicate high vegetation density while the precipitation amount indicates otherwise. This inconsistency between the observed precipitation and the observed canopy leaf density triggers the possibility that the observed high leaf density is due to an alternate source of water, irrigation.

We explore an inverse process approach using observations from the Moderate Resolution Imaging Spectroradiometer (MODIS), climatological data, and the NASA's Simple Biosphere model, SiB2, to quantitatively assess water demand in a semi-arid agricultural land by constraining the carbon and water cycles modeled under both equilibrium (balance between vegetation and prevailing local climate) and non-equilibrium (water added through irrigation) conditions. We postulate that the degree to which irrigated lands vary from equilibrium conditions is related to the amount of irrigation water used.

We added water using two distribution methods: The first method adds water on top of the canopy and is a proxy for the traditional spray irrigation. The second method allows water to be applied directly into the soil layer and serves as proxy for drip irrigation. Our approach indicates that over the study site, for the month of July, spray irrigation resulted in an irrigation amount of about 1.4 mm per occurrence with an average frequency of occurrence of 24.6 hours. The simulated total monthly irrigation for July was 34.85 mm. In contrast, the drip irrigation resulted in less frequent irrigation events with an average water requirement about 57% less than that simulated during the spray irrigation case. The efficiency of the drip irrigation method rests on its reduction of the canopy interception loss compared to the spray irrigation method. When compared to a country-wide average estimate of irrigation water use, our numbers are quite low. We would have to revise the reported country level estimates downward to 17% or less.

The numbers estimated from this work reflect an ideal physiologically-based target for efficient irrigation practices and could provide an objective basis for irrigation water use, especially in those regions where water is already scarce.

Editorial Manager(tm) for Remote Sensing of Environment
Manuscript Draft

Manuscript Number:

Title: Irrigation requirement estimation using MODIS vegetation Indices and inverse biophysical modeling A Case Study for Oran, Algeria

Article Type: Full length article

Section/Category:

Keywords: Irrigation; Modeling; MODIS; Semi-arid; Algeria

Corresponding Author: Research Scientist Lahouari Bounoua, B.S., M.S, Ph.D

Corresponding Author's Institution: NASA's Goddard Space Flight Center

First Author: Lahouari Bounoua, B.S., M.S, Ph.D

Order of Authors: Lahouari Bounoua, B.S., M.S, Ph.D; Marc L Imhoff, B.S., M.S, Ph.D; Shannon Franks, B.S., M.S.

Manuscript Region of Origin:

Irrigation requirement estimation using MODIS vegetation Indices and inverse biophysical modeling

A Case Study for Oran, Algeria

L. Bounoua, M. L. Imhoff and S. Franks

Abstract

We explore an inverse modeling process using the Simple Biosphere model-SiB2 forced by satellite observed biophysical data and climatological data to quantify water demand in a semi-arid agricultural area by constraining the carbon and water cycles modeled under both equilibrium, balance between vegetation and prevailing local climate, and non-equilibrium, water added through irrigation, conditions. We postulate that the degree to which irrigated dry lands vary from equilibrium climate conditions is related to the amount of irrigation water used. The amount of water required over and above precipitation is considered as an irrigation requirement.

We added water using two distribution methods: The first method adds water on top of the canopy and simulates the traditional spray irrigation. The second method allows water to be applied directly into the soil layer and serves as proxy for drip irrigation.

Results show that for the month of July, spray irrigation resulted in an additional amount of water of about 1.4 mm per occurrence with an average frequency of occurrence of 24.6

hours. The simulated monthly irrigation for July was 34.85 mm. In contrast, the drip irrigation resulted in less frequent irrigation events, about every 48 hours, with an average water requirement amount of 0.6 mm per occurrence or about 43% of that simulated during the spray irrigation case. The simulated total monthly irrigation under this method for July is 8.8 mm; a remarkable 26.05 mm less than the spray irrigation method. When compared to a country-wide average estimate of irrigation water use, our numbers are quite low. According to our results, we would have to revise the reported country level estimates downward to 17% or less.

The numbers estimated from this work reflect an ideal physiologically-based target for efficient irrigation practices and could provide an objective basis for irrigation water use, especially in regions where water is already scarce.

Introduction

Human demand for products of photosynthesis strongly influences the water cycle through land transformation and the diversion and extraction of fresh water needed to support agriculture. Even though water is abundant on our planet only about 3% of it is fresh and even less than 1% of it is available for human use (Gleick, 1996). Most (approximately 70%) of what is available is used for irrigation and agriculture followed by the industrial sector using around 22% while only 8% is left for all domestic use. With the growing demand for food and fiber, the scarcity of available fresh water is the subject of conflicts where political boundaries dissect natural watersheds and aquifers. It is expected that even if present water consumption remains unchanged, about 66% of the world population will live in water stressed conditions by 2025 (UNEP, 1996).

Over the next 25 years, population growth and economic development alone will substantially increase water demand and much of it for agricultural uses. For many regions on Earth, such as the semi-arid lands of central and northern Eurasia and North Africa, socio-economic shifts are likely to eclipse changes in mean climate as a driver of the future relation between water supply and demand (Vorosmarty et al., 2000). For these areas in particular, where the climatically driven balance between supply and demand is fragile, short-term variations in regional climate can have immediate and potentially predictable effect on agricultural production (Brown et al., 2007). Aside from monitoring stress, methodologies are needed that can measure and even predict

vulnerability to water scarcity based on a connection between land use and biophysical response to climate.

Climate, soil properties, crop type and agricultural practices are some of the primary factors influencing water demand both in terms of the source of water and amount used. A powerful way to quantify the interaction between climate, plant growth, and water resource requirements is the use of satellite observations and supporting biophysical modeling and climate data (Bounoua et al., 2000; Bounoua et al., 2002). Biophysical models can provide quantitative estimates of carbon and water flux as a function of satellite-derived vegetation parameters such as plant functional type, canopy structure, and leaf area in combination with data on soil properties and climate.

Here we explore an inverse process approach using observations from the Moderate Resolution Imaging Spectroradiometer (MODIS), climatological data, and the Simple Biosphere model SiB2 of Sellers et al. (1996a) to quantitatively assess water resource demand in a semi-arid agricultural area by constraining the carbon and water cycles modeled under both equilibrium (balance between vegetation and prevailing local climate) and non-equilibrium (water added through irrigation) conditions. We postulate that the degree to which irrigated dry lands vary from equilibrium conditions is related to the amount of irrigation water used.

Methodology

The method begins with the realistic assumption that, in its "natural" state vegetation density is in quasi-equilibrium with its local climate, soil and nutrient resources (Bounoua et al., 2004). Satellite driven land surface models, such as SiB2 and others, have proven useful for quantifying water and carbon flux for vegetated land cover in this equilibrium state (Dickinson et al., 1984; Sellers et al., 1996a; Sellers et al., 1997). In SiB2, the photosynthetic activity of the quantity of living vegetation indicated by the satellite data is modulated by the local climatology in a way that is consistent with observations and ecological theory of resource use efficiency (Cowan, 1977). However, irrigated agricultural lands in arid and semi-arid areas are not in equilibrium with the local climate. As such, despite the high satellite vegetation index (VI) observed for these areas, the modeled photosynthetic activity will be "suppressed" by the lack of adequate precipitation provided by that climate (Pongratz et al., 2006; Imhoff et al., 2004). We postulate that the degree to which the satellite observed vegetation indices of irrigated lands vary from what would be expected under equilibrium conditions is related to the amount of irrigation water used. Given the cover type, by inverting the satellite driven biophysical model, it is possible to explore the relationship between observed vegetation Leaf area index (LAI) in the equilibrium state and the amount of additional water required to deviate from it by increasing the water input in the model as a unique function of the root zone water content.

For this study we used the MODIS 1 km Leaf area index 16-day composite (MOD15A2) to describe the vegetation phenology and climate data to drive the biophysical model for the year 2005. The climate data required to drive the Simple Biosphere model consisted

of surface shortwave and long wave radiations, surface wind speed and temperature and large scale and convective precipitation. The climatological climate data were obtained from the National Center for Environmental Prediction (NCEP) reanalysis.

The Simple Biosphere Model

We used the Simple Biosphere model-SiB2 (Sellers et al., 1996a) for the inverse modeling component in this study. In SiB2, the vegetation distribution (Defries & Townshend 1994) as well as its spatial and temporal phenology is described using global satellite observations (Sellers et al., 1996b). Each vegetation class is assigned a set of parameters including: 1) time-invariant parameters such as morphological and optical properties and 2) time-varying physiological parameters describing the vegetation's phenology. In the version of SiB2 used in this study, we obtain LAI from the MODIS instrument (MOD15A2) to derive the biophysical fields such as the fraction of photosynthetically active radiation absorbed by the green leaves of the canopy (FPAR), the greenness fraction, the roughness length, the zero-plan displacement and the vegetation bulk aerodynamic resistance needed for the model (Sellers et al., 1996b). Fpar is used directly in an integrated photosynthesis-conductance model (Collatz et al., 1991, 1992) to calculate the photosynthesis and transpiration rates. Fpar is prescribed from satellite observations; it then affects the surface water and energy balance but does not respond to it. The LAI is used in the calculation of albedo as well as the transpiration and interception loss components of the evapotranspiration. Vegetation physiology also responds to climate conditions, mostly temperature and precipitation. Therefore a

perturbation to the either the climate or the physiological drivers is expected to result in a positive or negative feedback depending on the intensity of the perturbation. For example, an increase in LAI will produce more leaves on the canopy and will increase fpar which in turns increases photosynthesis, conductance to water and transpiration. If the increase in LAI however is not consistent with the amount of water available for plant's photosynthesis, it will cause the stomata to close and so result in water stress. The model photosynthetic uptake of CO_2 from the atmosphere is coupled with a water loss from the leaf interior and from soil water trough the stomates. The capacity of vegetation to convert soil moisture into latent heat flux is determined by the vegetation density, leaf area index, and stomatal conductance. The former is derived from satellite data and prescribed while the latter depends on atmospheric conditions and the amount of water available in the root zone, thus establishing the required strong and realistic coupling between the climate forcing and the soil hydrology. The photosynthetic-conductance sub-model is controlled by a soil moisture stress factor that reduces the carbon assimilation and consequently conductance and transpiration when root zone water is below a vegetation type dependant threshold. The water stress function depends on the root zone soil moisture potential and the critical water potential as defined by (1), both of which are soil and biome type dependent.

$$f(w_2) = \frac{1}{1 + e^{0.02(\psi c - \psi r)}} \qquad (1)$$

Where w_2 is the soil moisture in the root zone layer expressed as a fraction of saturation, ψ_c and ψ_r represent the critical water potential and the root zone soil moisture potential

expressed in meters, respectively; and where $\psi_r = \psi_s w_2^{-b}$ with ψ_s being the soil moisture potential at saturation and b an empirical parameter (Sellers et al., 1996a). The soil moisture stress function is then used to scale photosynthesis and the stomatal conductance. In SiB2, the water stress varies between 1 and 0, with 1 representing no stress. It inhibits photosynthesis by half when the soil moisture potential reaches the critical value.

The critical part of the model that is of interest to this study is its hydrology. The SiB2 hydrological module distributes the incoming precipitation into a canopy interception component and a through fall component. The canopy interception can either evaporate at potential rate or contribute to the through fall when canopy holding capacity is exceeded. The combination of the direct through fall and water dripping from the canopy is added to the ground liquid water store. There, the water can either evaporate or infiltrate into a shallow surface layer if the ground storage capacity is exceeded. If the infiltration rate is in excess of the infiltration capacity of the soil, the excess water contributes to surface runoff. Similarly water from the surface layer can either evaporate or infiltrate into the root zone layer from which it can be used by plants for transpiration through photosynthesis, flow back up into the surface layer, contribute to runoff or infiltrate into the deep soil layer. From the deep soil layer water can diffuse up to the root zone or contribute to runoff though drainage (Fig. 1).

Model Inversion for Estimation of Water Balance, Irrigation Water Volume, and Vulnerability

To explore the potential vulnerability of an area with respect to water resources, we invert the SiB2 photosynthesis-conductance model and examine the relationship between climate and the water stress function for a local semi arid land using observed vegetation phenology. For each time step under the prevailing climatology the value of the soil moisture potential is compared to the critical value, and water is added as needed to the prevailing climatology to reduce the water stress following the stream of procedure illustrated in Figure 2. Water input through precipitation is increased over and above the amount of observed precipitation until the water stress function is minimized. This provides a lower bound for the amount of additional water input required to sustain the canopy leaf density. It is important to note that over the test region there was no rainfall during the 2005 summer and therefore the amount of water added was exactly that needed to sustain the vegetation density. We define the critical minimum water stress value as the value allowing normal physiological activity under normal rainy conditions when the vegetation physiological activity is not stressed. For most crop types, this critical value is about 0.9 and corresponds to about 80 to 85% of the maximum assimilation rate. For water stress values below this critical threshold, vegetation undergoes some inhibition of the assimilation rate. However, assimilation can also be reduced by high temperatures even under irrigated conditions.

Discussion and Results: a case study for Oran, Algeria

Satellite data were used to estimate the biophysical fields of a crop canopy in Oran, a semi-arid region in the North African country of Algeria for the year 2005. In our simulations, the cropland is assigned SiB2 land cover type 12 corresponding to cropland /C3-grasses. Fields of observed leaf area index (MOD15A2) from MODIS were used to compute the fraction of the photosynthetically active radiation, the greenness fraction, the bulk aerodynamic resistances for vegetation, and the roughness length at 16-day interval. The site is located at around 35° 40'N, 0° 45'W and its climate is typically characterized by moderately wet, cool winters and dry, warm summers. The annual climatological precipitation is around 400 mm occurring mostly between October and May and the monthly mean temperatures range between 5°C to 15°C in winter and 15°C to 30°C in summer (WMO). The growing season over this region parallels the precipitation; however vegetation activity is completely inhibited during the dry summer. The site is selected to test the newly developed algorithm because of data availability and most importantly because there is an evident discrepancy between the observed high leaf area index during the summer and the precipitation distribution, thus suggesting irrigation.

The normal course of the phenology represented by the observed LAI is presented in Figure 3; whereas the climatological precipitation and the modeled water stress are shown in figure 4. The LAI time series shows an annual cycle with relatively high values except for a short period between February and the middle of March corresponding to the harvesting of cool weather crops. Remarkably however, during the summer when no rainfall is recorded (Figure 4) there is still a significantly high LAI value suggesting that the cropland is irrigated. Most irrigation over the region uses ground water withdrawals

from aquifers. The observed precipitation shows the last rainfall occurrence by mid-June and no rainfall occurrence during the month of July while the simulated water stress indicates maximum stress (low value) starting around the end of June. We use this inconsistency between the observed phenology and precipitation to both identify the need for supplemental water and quantify the minimum amount needed to sustain the observed LAI and the photosynthetic function of the crops. We focus our discussion on the month of July as it is the driest month over the region and discuss two irrigation scenarios that we compare to a control simulation.

The water stress for this canopy, without irrigation, is shown as a control (Figure 4) along with the observed precipitation. It is interesting to note that the last significant rainfall event before summer (0.38 mm hr^{-1}) occurs on June 24 and was associated with a low water stress value of 0.97. It took about 20 days after that date for the water stress function to drop to 0.25 (high stress) on July 15. Following this rainfall, the stomatal conductance and assimilation rates were maintained relatively high during the beginning of the month, then started to decline progressively to an almost complete inhibition at the end of the month (Figure 5).

The soil moisture content in the shallow surface layer is rather a fast response variable and drops to a constant low value soon after the last rainfall. In contrast, the root zone water content exhibited a slow decline (Figure 6).. The root zone depth for cropland is specified to a maximum 1 m to include several types of crops; and the actual amount of water in the layer is expressed as a fraction of saturation. Crop rotation is a common

practice for the study site, ranging from cool weather crops during early fall to wheat which usually starts by mid-November over this region. During summer, tall leafy crops are dominant. Examination of the assimilation rate and the root zone soil moisture illustrates the tight interplay between the two model variables and shows the assimilation rate closely following the root zone soil moisture. There was no rainfall during July and consequently the only water diffused to the atmosphere was extracted by plants from the root zone during the process of photosynthesis. Because the assimilation remains positive for this relatively dense canopy under a long period with no precipitation, we conclude that during the control simulation, the model's vegetation physiological activity is not in balance with its local climate.

It is the inconsistency between the observed precipitation and the observed canopy leaf density that triggers the hypothesis that the observed high leaf density is due to an alternate source of water resources possibly through irrigation. In addition to identifying a potentially irrigated canopy, we then used the SiB2 biophysical model to estimate the amount of water needed to sustain the observed LAI (figure 3) at its high point under local climate conditions. Water is then added as needed at each time step during daytime where the model computed water stress is below the critical value indicating that the water content in the root zone can not sustain an unstressed level of photosynthesis between 12-13 μmoles.m^{2}.s^{-1}, typical for the cropland in this semi arid region. The amount of water required over and above precipitation (if any) is considered as an irrigation requirement.

We added water using two distribution methods: The first method, hereafter referred to as *exp1*, adds water similar to large scale rainfall; that is the water is added on top of the canopy and covers the entire grid cell uniformly. This implies that some of the irrigation water is intercepted by the canopy and is lost back to evaporation at potential rate. This method is a proxy for the traditional spray irrigation. The second method, referred to as *exp2*, allows water to be applied directly into the first soil layer and serves as good proxy for modern drip irrigation.

The response of the water stress function to irrigation for *exp1* is shown in Figure 7a. Irrigation has maintained a water stress level slightly above the 0.9 threshold and provided a maximum amount of about 1.4 mm of water per occurrence with an average frequency of occurrence of 24.6 hours. The simulated total monthly irrigation for July is 34.85 mm. The minimum and maximum temperatures averaged for June, July and August over the study site are 19.7 °C and 33.44 °C, respectively and the water vapor deficit is high. The additional irrigation had an important effect on the surface water and energy budgets. Since water is added directly on top of the canopy, it first saturates the canopy interception store, fills the surface layer and then infiltrates into the root zone. The water content in the first layer almost mirrors the irrigation pattern. This is due to this layer's relatively small water holding capacity. As water is added however, the moisture content in the root zone slowly builds up and maintains values significantly higher than those obtained during the control simulation (Figure 7b). Since both the canopy and the soil are wet during and after irrigation, water is lost to the atmosphere through interception, especially from the canopy which is exposed to high atmospheric

temperatures and vapor pressure deficit (Figure 8). This result in cooling and moistening the canopy air space; however at this spatial scale evaporation does not have a significant effect on local climate.

The high temperatures reached during daytime in this semi arid region have an adverse impact on assimilation (Figure 9). For example between about July 13 and 27, the assimilation rates is not as strong as the first 10 days of the month due to high temperatures, nevertheless the irrigation resulted in a higher productivity than the control case.

During the second simulation (*exp2*) where water is added directly to the soil, the irrigation is much more efficient than in *exp1*. The drip irrigation reduced the interception loss from the canopy by a monthly average value of 4.93 Wm^{-2} or about 24% compared to the spray irrigation case; and because the ground is covered by thick foliage, the ground interception is relatively small. In both experiments, however the ground transpiration underwent a significant increase compared to the control. This partitioning of the surface fluxes shunted a large part of the absorbed energy into canopy transpiration which increased by about 6.5 Wm^{-2} compared to *exp1* and almost doubled from the control value (Table1). The use of the drip irrigation method results in less frequent irrigation events (about every 48 hours) with an average water requirement amount of about 0.6 mm per occurrence, that's about 43% of that simulated during the spray irrigation case (Figure 10). The simulated total monthly irrigation under this method for July is 8.8 mm; that is a remarkable 26.05 mm less than *exp1*.

Concluding Remarks

The model approach provided minimum water requirements for sustaining this canopy under prevailing climate conditions. The proxy for spray irrigation (*exp1*) yielded a minimum water requirement of 117 mm of water per square meter (per year) while the more economic proxy for drip irrigation (*exp2)* yielded a minimum requirement of 30 mm per square meter (per year). As expected, when compared to a country-wide average estimate of irrigation water use for Algeria, our numbers are quite low (Table 2). Since our results are based on model physiology they represent perfect water delivery efficiency and do not include losses due to transport of the water to the plants. In actual practice, a considerable amount of water is lost in transport and while this is factored into calculations of irrigation efficiency it represents a large source of uncertainty in the estimates. The range of irrigation efficiencies between 45 and 80% (UNFAO) reported for Algeria represents an average gross irrigation figure and probably includes some regions in the Sahara desert. Our results apply only to one coastal region away from the desert. Nevertheless, according to our results, we would have to revise the reported country level estimates downward 17% or less. The numbers estimated from this work reflect an ideal physiologically-based target for efficient irrigation practices and could provide an objective basis for irrigation water use, especially in those regions where water is already scarce.

These experiments lay the ground work for using satellite derived canopy measures and biophysical models to assess irrigation requirements and irrigation water use efficiency regionally. The approach provides a physiological baseline requirement to which reported irrigation water use can be compared in order to improve both estimates and delivery systems. The technique can also be expanded to assess water vulnerability of both crops and natural ecosystems as a result of climate change.

Acknowledgement

This work was partially funded by the NASA Land Cover Land Use Change (LCLUC) program, G. Gutman.

References

Bounoua, L., Collatz, G.J., Los, S., Sellers, P.J., Dazlich, D.A., Tucker, C.J. & Randall, D.A. (2000). Sensitivity of climate to changes in NDVI. *Journal of Climate*, 13, 2277-2292.

Bounoua, L., DeFries R.S., Collatz, G.J., Sellers, P.J., & Khan, H. (2002). Effects of land cover conversion on surface climate. *Climate Change*, 52, 29-64.

Bounoua L., Defries, R. S., Imhoff, M. L. & Steininger, M. K. (2004). Land use and local climate: A case study near Santa Cruz, Bolivia. *Meteorology and Atmospheric Physics*, 86, 73-85.

Brown M.E., Funk, C., Galu, G. & Choularton, R. (2007) Earlier Famine Warning Possible Using Remote Sensing and Models. *EOS Transactions of the American Geophysical Union*, 88, 381-382.

Collatz, G. J., Ball, J. T., Grivet, C. & Berry, J. A. (1991). Physiological and environmental regulation of stomatal conductance, photosynthesis and transpiration: a model that includes a laminar boundary layer. *Agriculture and Forest Meteorology*, 54, 107-136.

Collatz, G.J., Ribas-Carbo, M. & Berry, J.A. (1992). Coupled photosynthesis-stomatal conductance model for leaves of C4 plants. *Australian Journal of Plant Physiology*, 19, 519-538.

Cowan, I. R. (1977). Stomatal behavior and environment. *Advances in Botanical Research,* 4**,** 117–228.

DeFries, R. S & Townshend, J. R. G. (1994). NDVI-derived land cover classifications at a global scale. *International Journal of Remote Sensing*, 15, 3567-3586.

Dickinson, R. E. (1984). Modeling Evapotranspiration for Three-Dimensional Global Climate Models. In J. E. Hansen and T. Takahashi (Eds.), *Climate Processes and Climate Sensitivity* (pp. 58–72). Washington D.C: Geophysical Monograph 29, American Geophysical Union

Gleick, P. H. (1996) Water resources. In S. H. Schneider (Ed.), *Encyclopedia of Climate and Weather,* Vol. 2 (pp.817-823). New York: Oxford University Press

Imhoff, M. L., Bounoua, L., Lawrence, W.T., Stutzer, D. & Ricketts, T. (2004). The consequences of urban land transformation on net primary productivity in the United States. *Remote Sensing of Environment*, 89, 434-443.

Pongratz, J., Bounoua, L., Defries, R. S., Morton, D. C., Anderson, L. O., Mauser, W. & Klink, C. (2006). The impact of land cover change on surface energy and water balance in Mato Grosso, Brazil. *Earth Interactions*, 10, 1–17.

Sellers, P, Mintz, Y, Sud, Y. & Dalcher, A (1986). A Simple Biosphere Model (SiB) for use within General Circulation Models, *Journal of Atmospheric Science,* 43, 505-531.

Sellers, P. J., Randall, D. A., Collatz, G. J., Berry, J. A., Field, C. B., Dazlich, D. A., Zhang, C., Collelo, G. D. & Bounoua, L. (1996a). A revised land surface

parameterization (SiB2) for atmospheric GCMs, Part 1: Model formulation. *Journal of Climate*, 9 (4), 676-705.

Sellers, P. J, Los, S. O., Tucker, C. J., Justice, C.O., Dazlich, D. A, Collatz, G. J. & Randall, D. A. (1996b). A revised land surface parameterization (SiB2) for atmospheric GCMs, Part 2: The generation of global fields of terrestrial biophysical parameters from satellite data. *Journal of Climate* 9 (4), 706-737.

Sellers, P. J., Dickinson, R. E., Randall, D. A., Betts, A. K., Berry, J. A., Collatz, G. J., Denning, A. S., Mooney, H. A., Nobre, C. A., Sato, N. & Field, C. B. (1997). Modeling the exchanges of energy, water, and carbon between continents and the atmosphere. *Science,* 275, 502-509.

UNFAO, http://www.fao.org/docrep/W4347E/w4347e0s.htm

United Nation Environmental Program (1996). Water for the Future: The West Bank and Gaza Strip, Israel, and Jordan (1999) Commission on Life Sciences (CLS). Report available at http://books.nap.edu/openbook.php?record_id=6031&page=54

Vörösmarty, C. J., Green, P., Salisbury, J. & Lammers, R. (2000). Global water resources: Vulnerability from climate change and population growth. *Science,* 289, 284-288.

World Meteorological Organization (WMO): data available at World Weather Information Service, Climatological information based on monthly averages for the 30-year period 1976-2005. Data available http://www.worldweather.org/

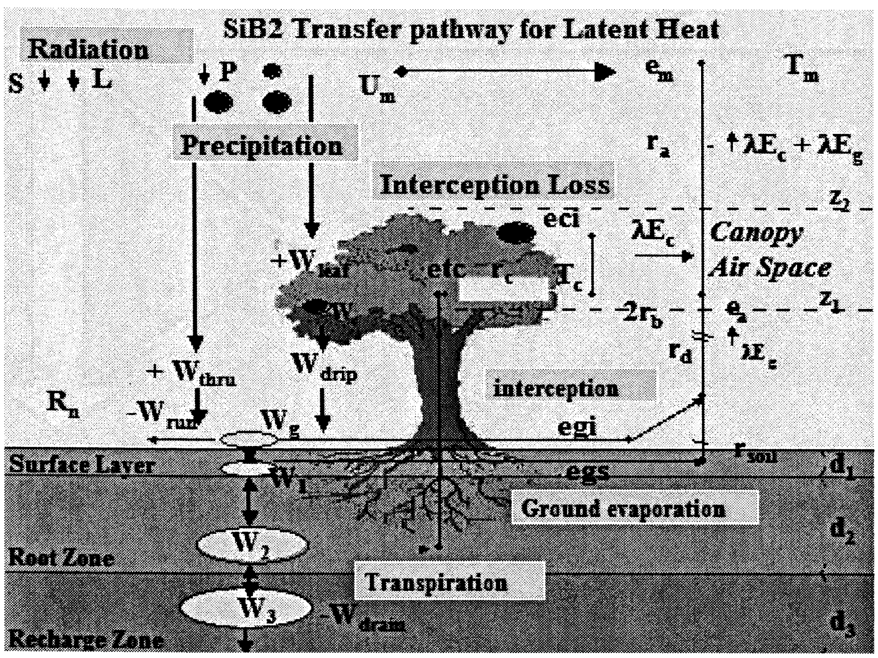

Figure 1: Schematic functioning of the Simple Biosphere Model (SiB2) showing the pathway for the hydrological cycle treatment.

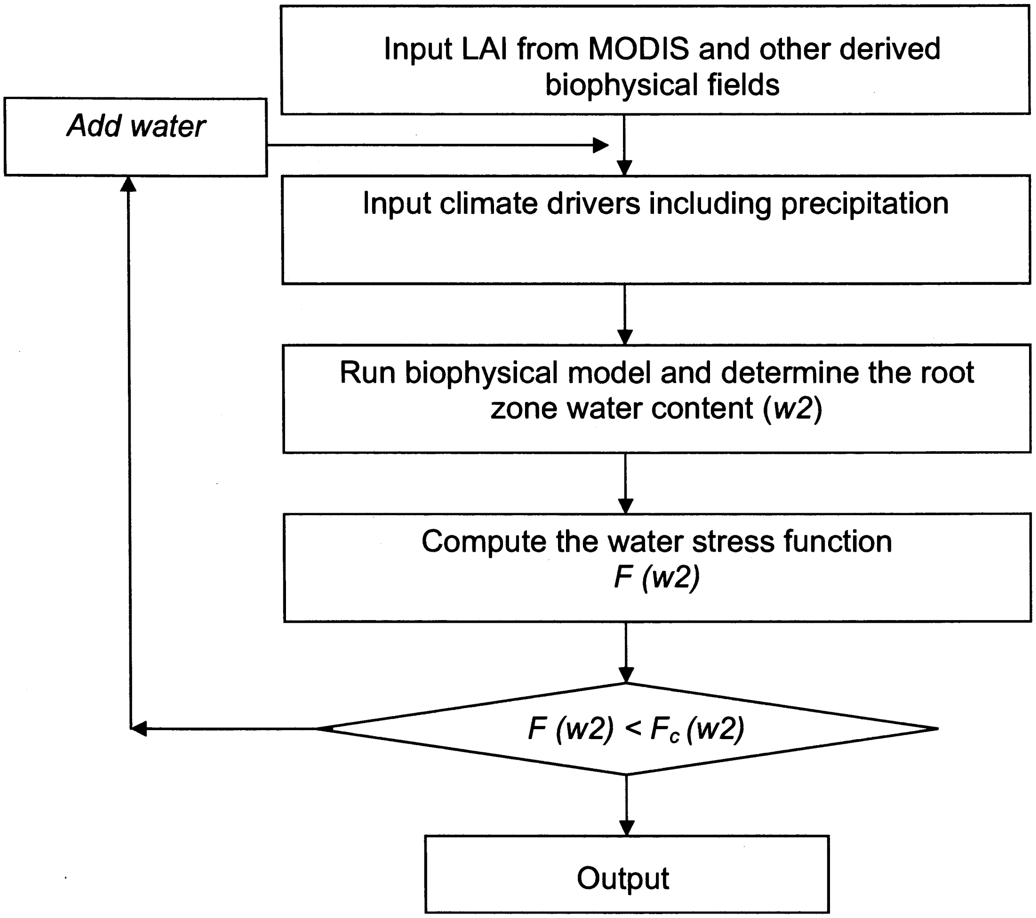

Figure 2: Iterative process for the determination of the minimum water required to sustain the observed leaf density on the vegetation canopy. Baseline in this case is the observed leaf area index (LAI) from MODIS (updated every 16 days) and local climatology (obtained hourly from daily observations), which includes precipitation. Water is added to reduce the water stress function. Output is the amount of water required to maintain that balance.

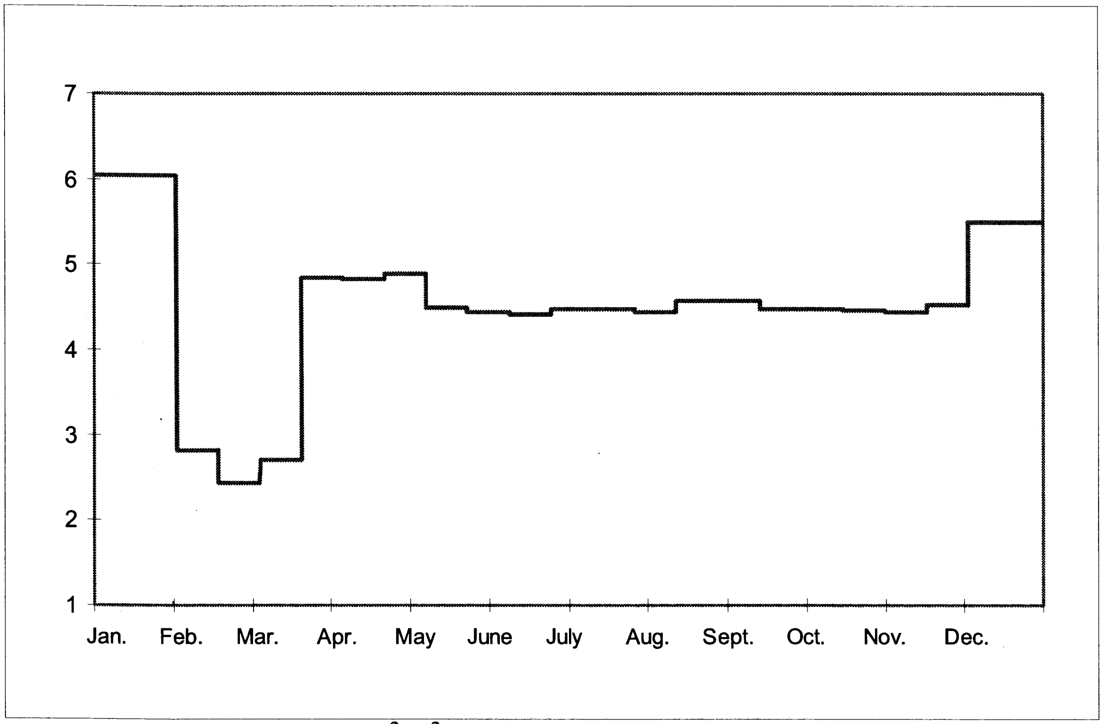

Figure 3: Leaf Area Index (m^2m^{-2}) as observed from MODIS for the study region.

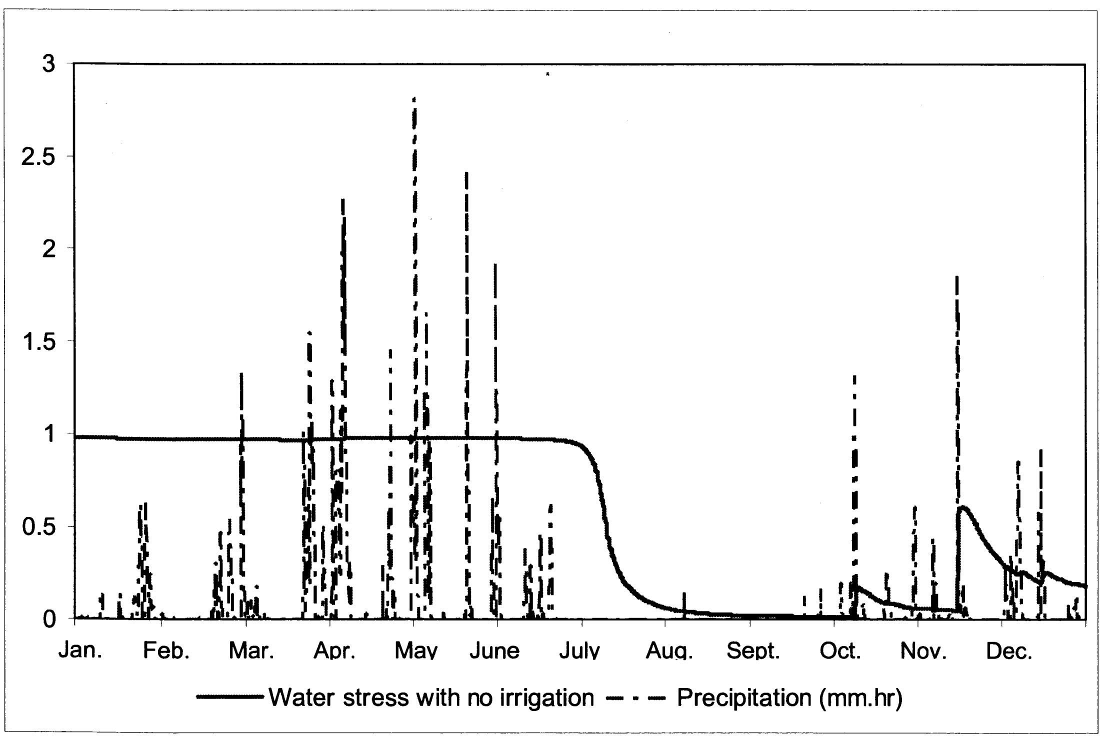

Figure 4: Hourly annual cycles of precipitation in $mm.hr^{-1}$ and water stress (dimensionless).

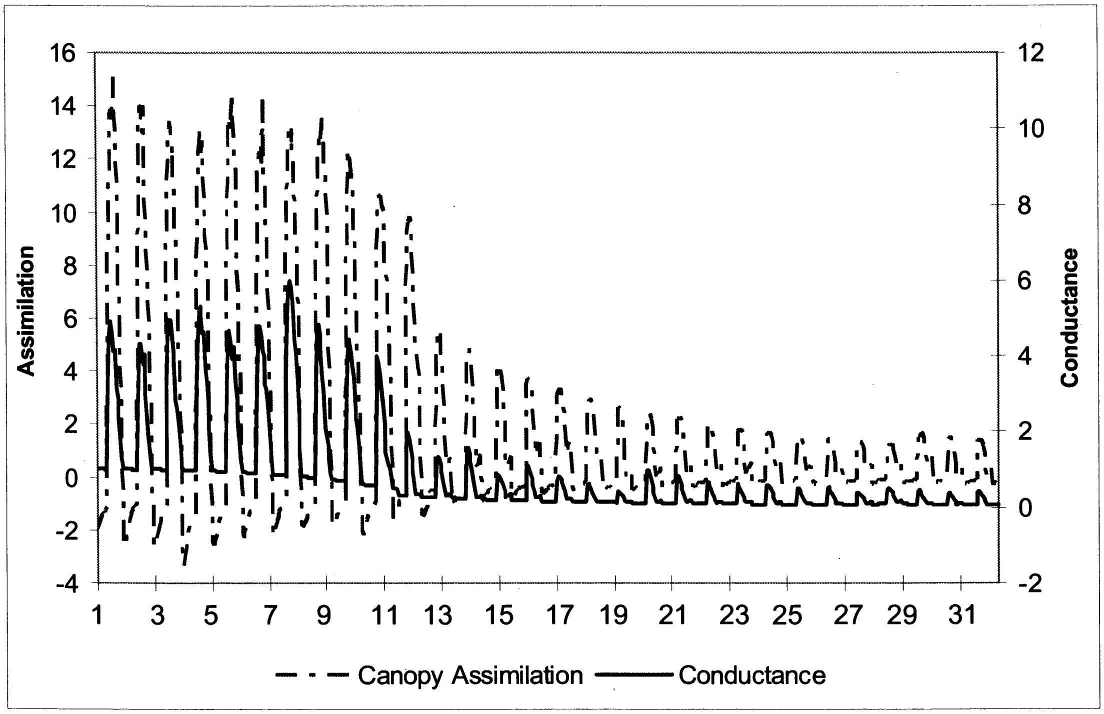

Figure 5: Assimilation in µmoles.$m^2.s^{-1}$ and stomatal conductance in $m.s^{-1}$, for the non-irrigated case in the month of July.

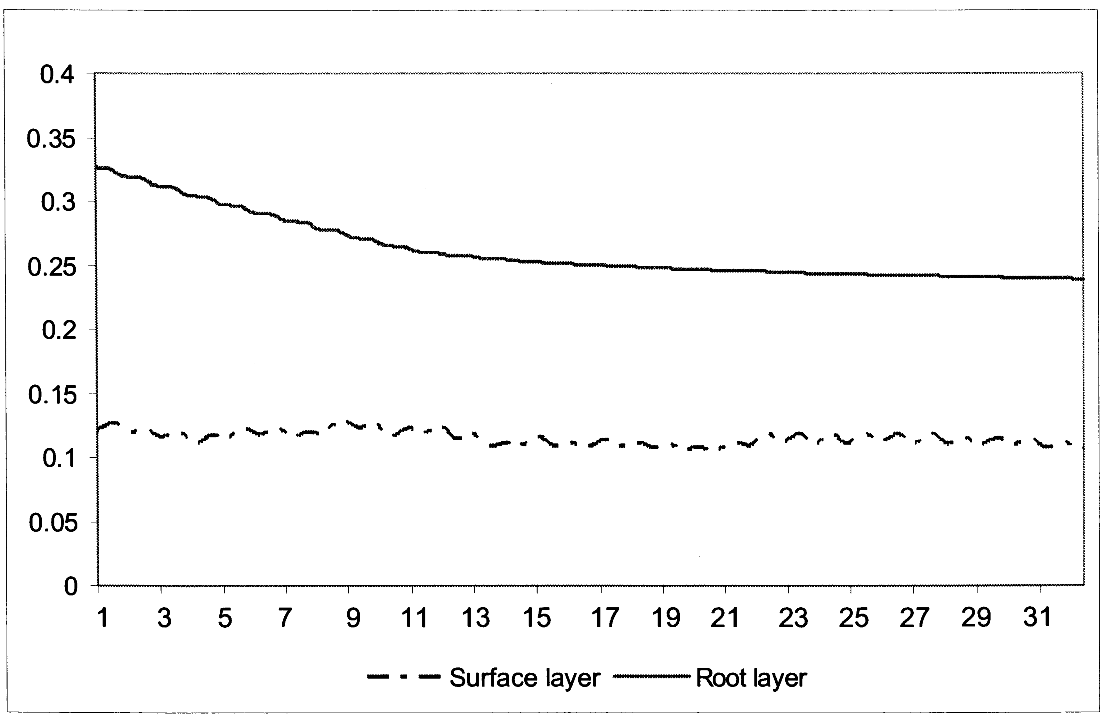

Figure 6: Surface and root zone layer soil water content for the month of July, expressed as percent of saturation.

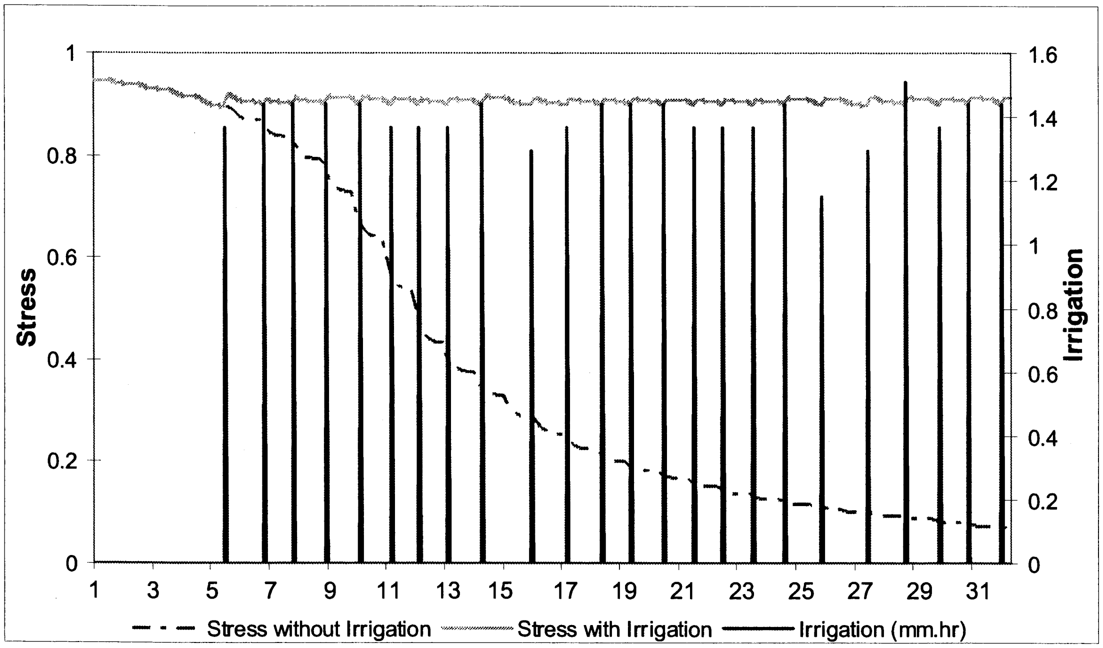

Figure 7a: Irrigation in mm.hr^{-1} for exp1; also shown is the water stress function (dimensionless) for exp1 and for the control, for the month of July

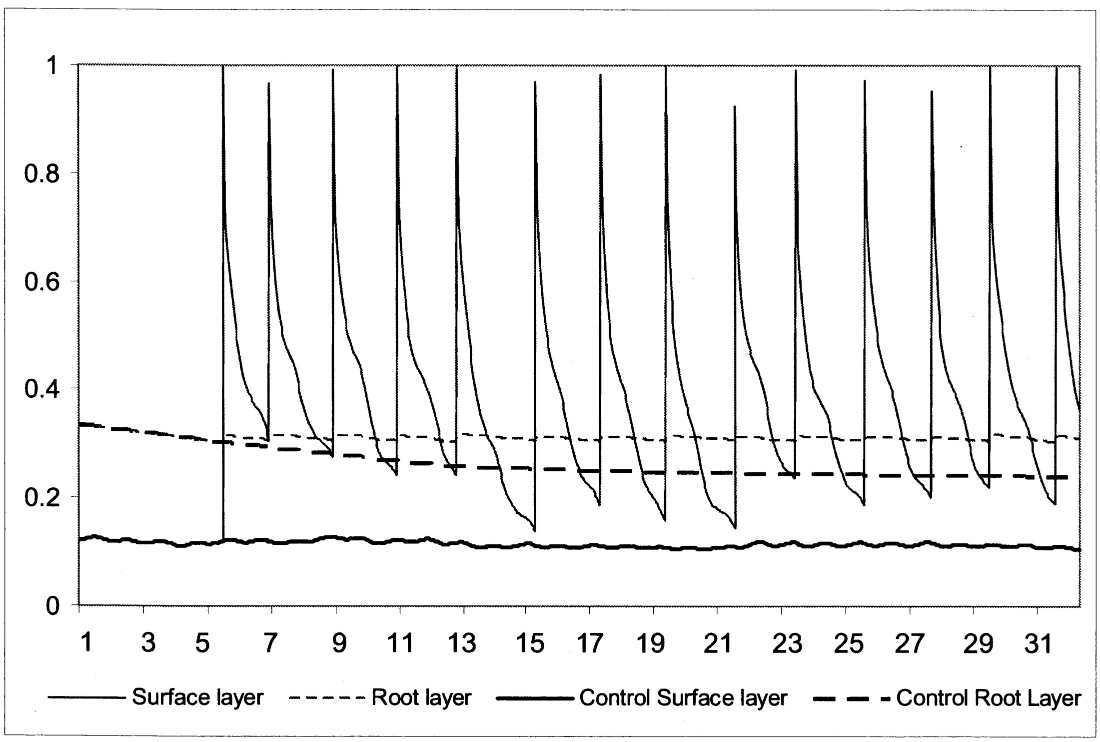

Figure 7b: Surface and root zone layer water content for exp1 and the control; expressed as a fraction of saturation, for the month of July.

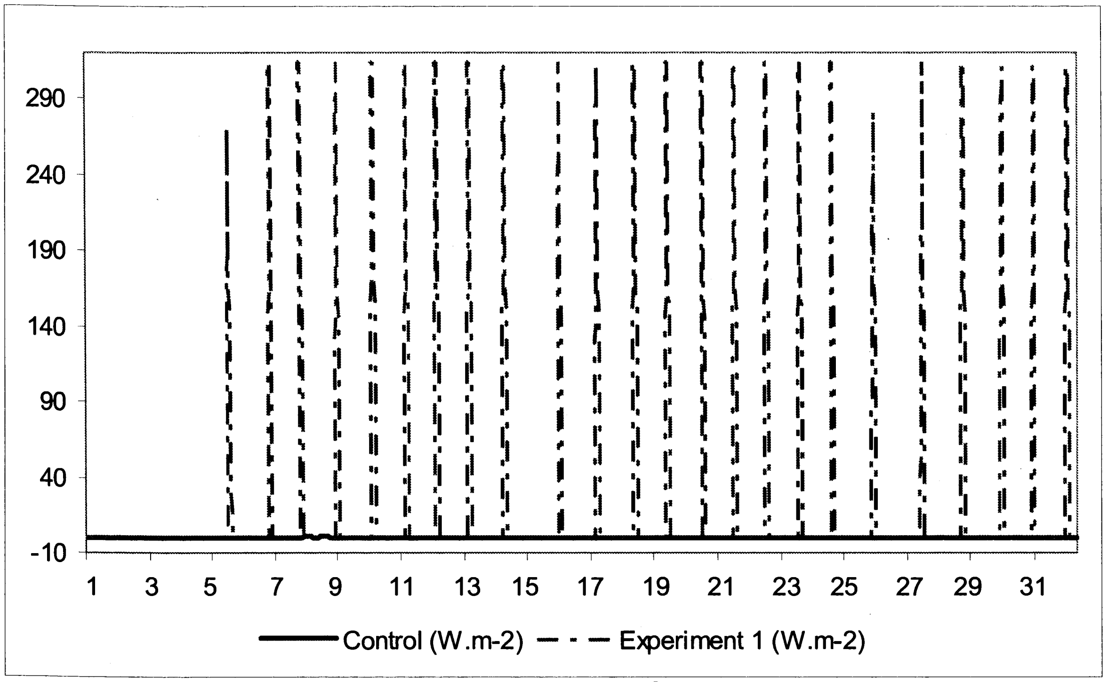

Figure 8: Canopy plus ground interception ($W.m^{-2}$) during exp1 in the month of July.

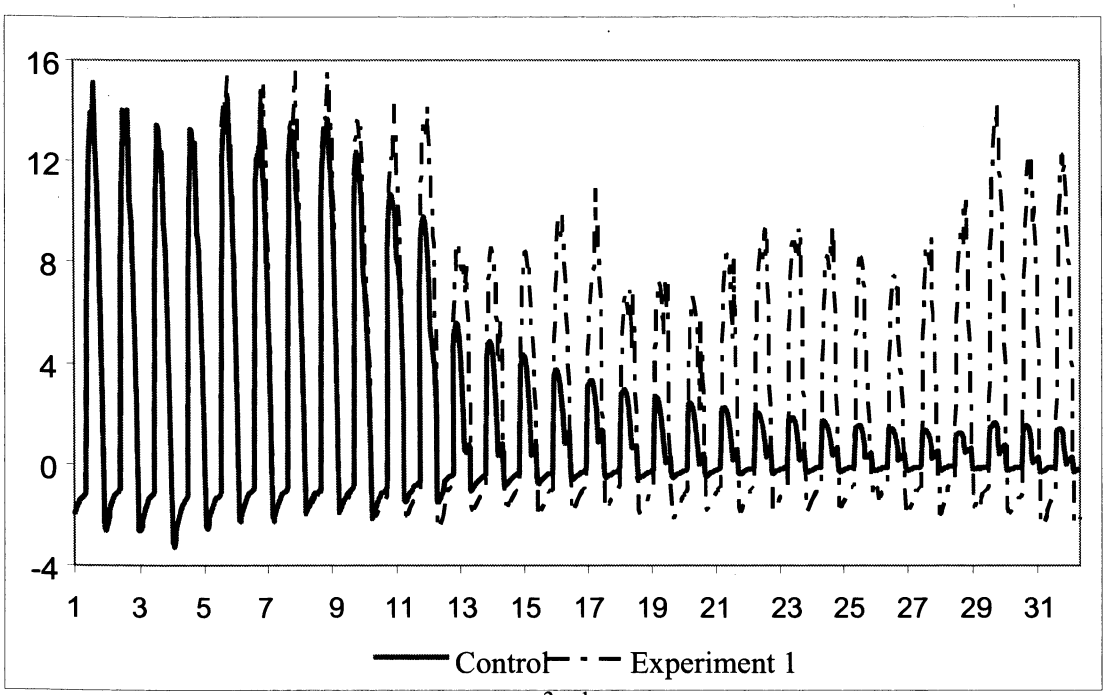

Figure 9: Assimilation rates in $\mu moles.m^{-2}.s^{-1}$ for control and exp1, for the month of July.

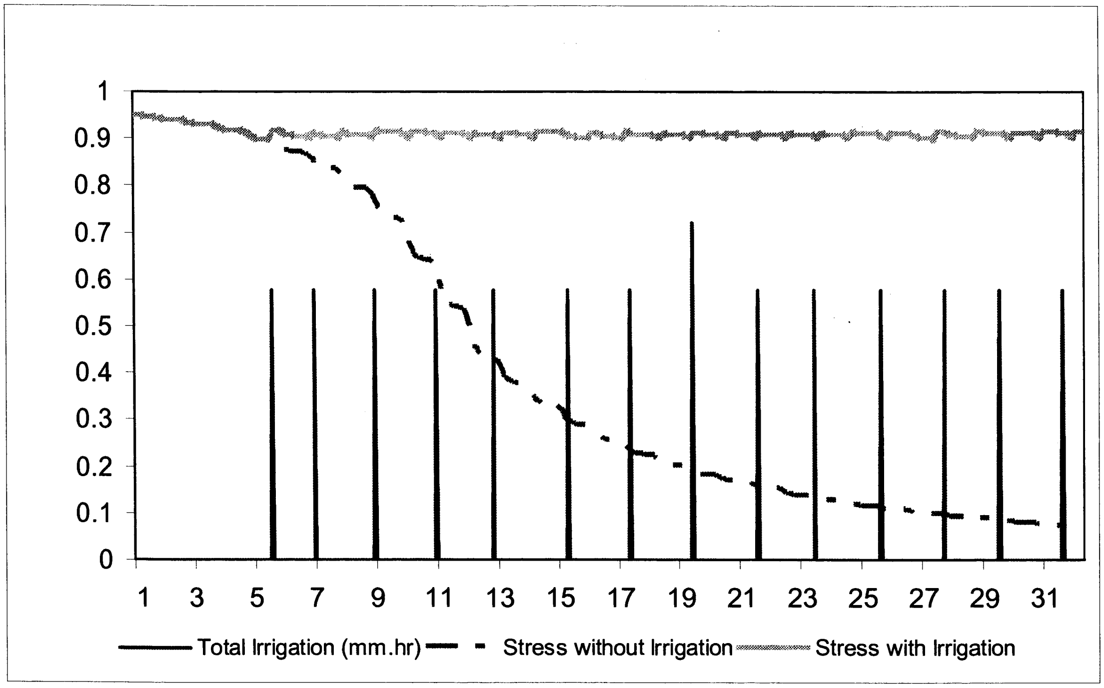

Figure 10: Irrigation in mm.hr^{-1} for exp2; also shown is the water stress function for exp2 and for the control. Data is for the month of July.

Table 1: Canopy and ground transpiration and interception components (W.m^{-2})

	Control	Exp1	Exp2
canopy transpiration	41.64	73.98	80.46
ground transpiration	1.47	41.64	74.61
canopy interception	0.02	20.59	15.66
ground interception	1.36	1.87	4.29

Table 2: Water requirements as determined by exp1 and exp2 compared to reported estimates at country level for Algeria. (UNEP, 1996).

	Water Delivery	Water requirement (mm.m^{-1}.yr^{-1})
UN FAO*	Irrigation (All types)	700
EXP 1	Spray Irrigation	117
EXP 2	Drip Irrigation	30